

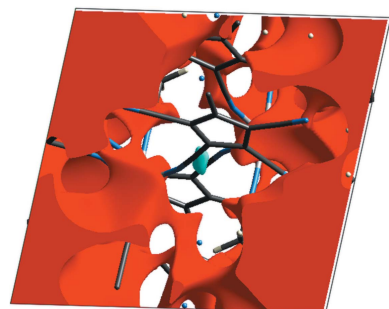
Received 1 September 2021  
Accepted 11 January 2022

Edited by E. Reinheimer, Rigaku Americas Corporation, USA

**Keywords:** ferrocene; pentacyanocyclopentadienide;  $\pi$ - $\pi$  interactions; weak interactions; decacyanoferrocene; crystal structure.

**CCDC reference:** 2141277

**Supporting information:** this article has supporting information at journals.iucr.org/c



OPEN ACCESS

# Coordination chemistry of polynitriles. Part 9. Decacyanoferrocene revisited. Crystal and molecular structure of *cis*-[ $\{C_5(CN)_5\}_2(MeCN)_4Fe]$

Karlheinz Sünkel\* and Tobias Blockhaus

Ludwig-Maximilians-Universität München, Department Chemie, Butenandtstrasse 9, 81377 Munich, Germany.

\*Correspondence e-mail: suenk@cup.uni-muenchen.de

The reaction of  $Ag[C_5(CN)_5]$  with anhydrous  $FeCl_2$  in acetonitrile leads to colourless crystals of tetrakis(acetonitrile- $\kappa N$ )bis(pentacyanocyclopentadienido- $\kappa N$ )iron(II) acetonitrile 1.8-solvate,  $[Fe(C_{10}N_5)_2(CH_3CN)_4] \cdot 1.8CH_3CN$  or *cis*-[ $\{C_5(CN)_5\}_2(MeCN)_4Fe]$ ·1.8MeCN. The compound crystallizes in the triclinic space group  $P\bar{1}$  as monomers, which exhibit weak C–H $\cdots$ N and  $\pi$ - $\pi$  interactions. The crystals contain *ca* 20% solvent-accessible voids, which are nearly completely filled by two MeCN molecules.

## 1. Introduction

The term ‘decacyanoferrocene’ appeared first in a publication about ‘diazotetracyanocyclopentadiene’ (Webster, 1966) and later in two US patents by the same author (Webster, 1970, 1974). It was used for the reaction product from silver pentacyanocyclopentadienide and  $FeCl_2$  in acetonitrile, which led to ‘light-green crystals of decacyanoferrocene’, which were characterized, after drying at 112 °C under vacuum, by elemental analysis and IR and UV spectroscopy as ‘ $C_{20}N_{10}Fe \cdot xH_2O$ ’. No indication or proof was given for the formulation as a ‘ferrocene’. A couple of years later, a different research group repeated the experiment and described the primary product as ‘white crystals’ (Christopher & Venanzi, 1973). Drying of the crystals at room temperature *in vacuo* produced a white solid that still, according to its IR spectrum, contained acetonitrile. Further drying at 110 °C *in vacuo* produced a pale-yellow-green product, which analyzed as ‘ $C_{20}N_{10}Fe \cdot xH_2O$ ’ and was further characterized by IR spectroscopy and magnetic and conductivity measurements. In the absence of a crystal structure determination, these authors postulated a ‘polymeric structure in which the iron is in an approximately octahedral environment’, in which ‘each PP group bridges three iron atoms’. Within the last 15 years, the coordination chemistry of the pentacyanocyclopentadienide anion has been studied intensively by us and others (Sünkel & Reimann, 2013; Sünkel & Nimax, 2018; Nimax *et al.*, 2018; Blockhaus & Sünkel, 2021; Bacsa *et al.*, 2011; Less *et al.*, 2013). These studies showed that  $[C_5(CN)_5]^-$  could behave either as a noncoordinating anion or use one to its five cyano groups for coordination, sometimes even in a bridging  $\mu_2$ - $\kappa^1$ : $\kappa^1$  fashion. We had also treated  $FeCl_2$  with  $Ag[C_5(CN)_5]$  in methanol. Recrystallization from MeOH gave crystals of *trans*-[ $\{C_5(CN)_5\}_2Fe(H_2O)_4$ ], in which both anions used only one cyano function each for coordination to iron in a mononuclear compound (Sünkel *et al.*, 2019). Individual molecules were connected *via* hydrogen bridges into a three-dimensional

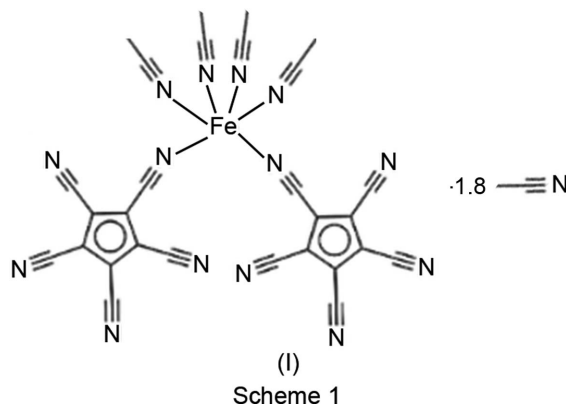
**Table 1**  
Experimental details.

	With localized solvent	With SQUEEZE
Crystal data		
Molecular formula	[Fe(C <sub>10</sub> N <sub>5</sub> ) <sub>2</sub> (C <sub>2</sub> H <sub>3</sub> N) <sub>4</sub> ]·1.8C <sub>2</sub> H <sub>3</sub> N	C <sub>28</sub> H <sub>12</sub> FeN <sub>14</sub>
Chemical formula	C <sub>31.6</sub> H <sub>17.4</sub> FeN <sub>15.8</sub>	600.37
<i>M</i> <sub>r</sub>	674.29	
Crystal system, space group	Triclinic, <i>P</i> ̄1	
Temperature (K)	109	
<i>a</i> , <i>b</i> , <i>c</i> (Å)	11.9972 (7), 12.8711 (7), 13.0907 (8)	
α, β, γ (°)	62.528 (2), 82.929 (2), 77.210 (2)	
<i>V</i> (Å <sup>3</sup> )	1748.47 (18)	
<i>Z</i>	2	
Radiation type	Mo <i>K</i> α	
μ (mm <sup>-1</sup> )	0.48	0.47
Crystal size (mm)	0.05 × 0.04 × 0.03	
Data collection		
Diffractometer	Bruker D8 Venture	
Absorption correction	Multi-scan ( <i>SADABS</i> ; Krause <i>et al.</i> , 2015)	
<i>T</i> <sub>min</sub> , <i>T</i> <sub>max</sub>	0.616, 0.745	
No. of measured, independent and observed [ <i>I</i> > 2σ( <i>I</i> )] reflections	17051, 7081, 5145	17056, 7083, 5145
<i>R</i> <sub>int</sub>	0.042	
(sin θ/λ) <sub>max</sub> (Å <sup>-1</sup> )	0.626	
Refinement		
<i>R</i> [ <i>F</i> <sup>2</sup> > 2σ( <i>F</i> <sup>2</sup> )], <i>wR</i> ( <i>F</i> <sup>2</sup> ), <i>S</i>	0.064, 0.163, 1.03	0.061, 0.141, 1.04
No. of reflections	7081	7083
No. of parameters	464	392
No. of restraints	3	0
H-atom treatment	H-atom parameters constrained	
Δρ <sub>max</sub> , Δρ <sub>min</sub> (e Å <sup>-3</sup> )	0.81, -0.63	0.77, -0.64

Computer programs: *APEX2* (Bruker, 2011), *SAINT* (Bruker, 2011), *SHELXT2014* (Sheldrick, 2015a), *SHELXL2018* (Sheldrick, 2015b) and *Mercury* (Macrae *et al.*, 2020).

network. Since all the above-mentioned reports described the formation of (either ‘light green’ or ‘white’) crystals as the primary product of the reaction in acetonitrile, we decided to repeat this reaction and to study the crystals.

crystals at 110 °C *in vacuo* for several hours left an amorphous powder. All attempts to obtain crystals of this product by dissolution in a noncoordinating solvent met with failure.



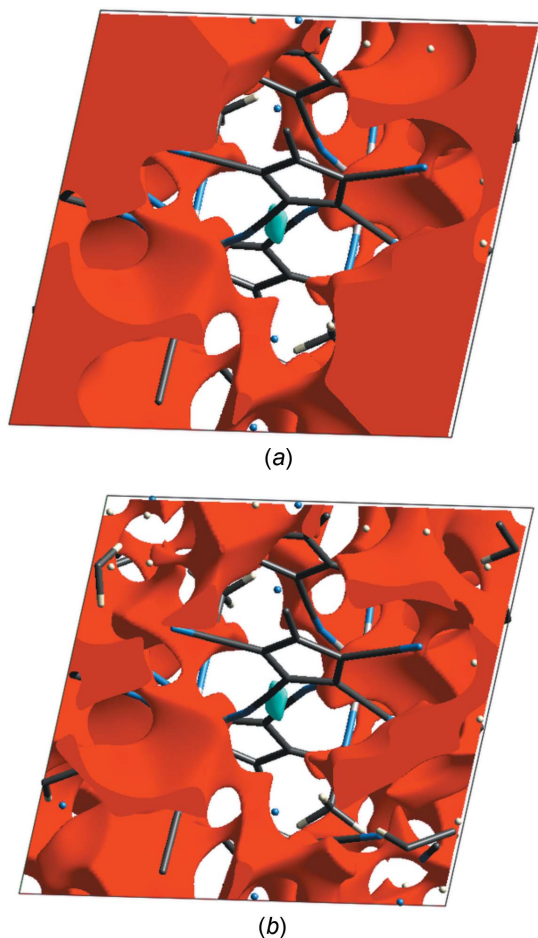
## 2. Experimental

### 2.1. Synthesis and crystallization

The title compound, tetrakis(acetonitrile-κ*N*)bis(penta-cyanocyclopentadienido-κ*N*)iron(II) acetonitrile disolvate, (I) (Scheme 1), was prepared as described in the literature (Webster, 1966; Christopher & Venanzi, 1973). Recrystallization of the crude product by slow evaporation of an acetonitrile solution under an argon atmosphere gave colourless crystals suitable for X-ray diffraction analysis. Heating the

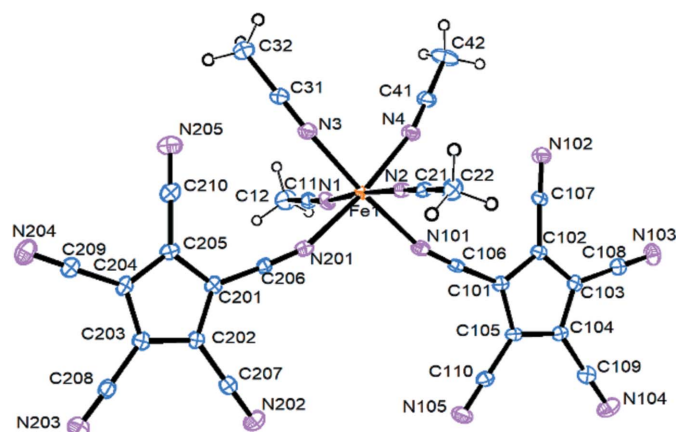
### 2.2. Refinement

The structure refinement showed, besides the molecular unit, two lattice acetonitrile (MeCN) molecules, which were both disordered. The disorder of one MeCN molecule could be resolved with the help of restraints into two positions in relative 80:20 occupancies. The disorder of the second molecule, however, could not be resolved. Due to some unfavourable close contacts with the ‘minor’ molecule, the site-occupancy factor (s.o.f.) of the second molecule was reduced to 0.8 anyway. After inclusion of these MeCN molecules, *PLATON* (Spek, 2020) analysis showed no more solvent-accessible voids. The results of the refinement using this model are shown in the second column of Table 1. As the *PLATON* analysis of the structure without the lattice acetonitrile molecules showed 20% solvent-accessible voids (for a ‘cavity plot’, see Fig. S1 of the supporting information), a refinement using the SQUEEZE routine (Spek, 2015) was tried. The results of this refinement are shown in the third column of Table 1. As can be seen, the SQUEEZE refinement led to slightly better *R* values. To obtain further insight into the importance of crystal voids in this structure, the ‘un-SQUEEZEd’ CIF file was examined using the program *CrystalExplorer* (Version 21.5), using the subroutine ‘void’

**Figure 1**

Crystal void plots (0.002 a.u. isosurface) of the crystal structure (a) without and (b) including the MeCN lattice molecules.

(Turner *et al.*, 2011), both without and with the acetonitrile molecules. Fig. 1(a) shows the void plot obtained without the MeCN molecules, while Fig. 1(b) shows the same plot when the MeCN molecules were included (0.002 a.u. isosurfaces; for the results of the corresponding calculations using 0.0003 a.u. isosurfaces, see Fig. S2 in the supporting information). Table 2

**Figure 2**

Displacement ellipsoid plot (30% probability level) of (I). The lattice MeCN molecules are not shown.

**Table 2**

Comparison of the void calculations using *PLATON* and *CrystalExplorer* (*CE*).

SASA is solvent accessible surface area (Düren *et al.*, 2007).

	<i>PLATON</i> VOID	<i>PLATON</i> SASA	<i>CE</i> (0.002 a.u.)	<i>CE</i> (0.0003 a.u.)
Without MeCN				
Void volume	346		473.4	191.0
Void surface		281	721.2	237.9
With 2MeCN				
Void volume	0		211.6	0.3
Void surface		0	716.4	3.2

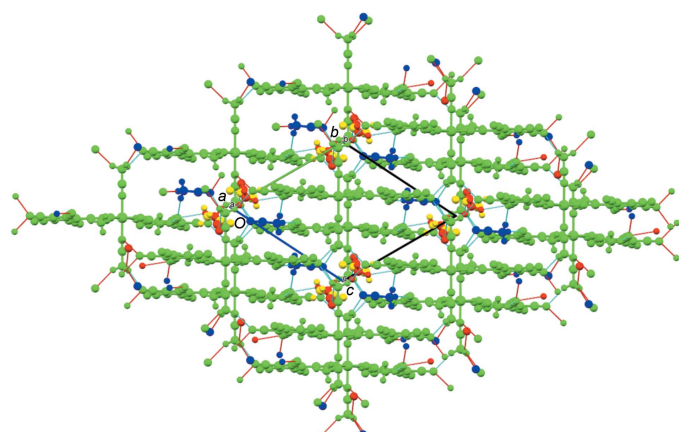
summarizes the results of the void-space calculations using *PLATON* and *CrystalExplorer*.

As can be seen, the results obtained with *PLATON* (excluding the MeCN solvents) are intermediate between the *CrystalExplorer* results with the two different isosurfaces, which is rather unusual (Turner *et al.*, 2011). After inclusion of the MeCN molecules, the *PLATON* results and the *CrystalExplorer* results for a 0.0003 a.u. surface are nearly identical, and show that there are no permanent voids left after inclusion of the MeCN molecules. In view of this, together with the probable involvement of the lattice MeCN molecules in C—H···N hydrogen bonds, the SQUEEZEd structure was not examined further.

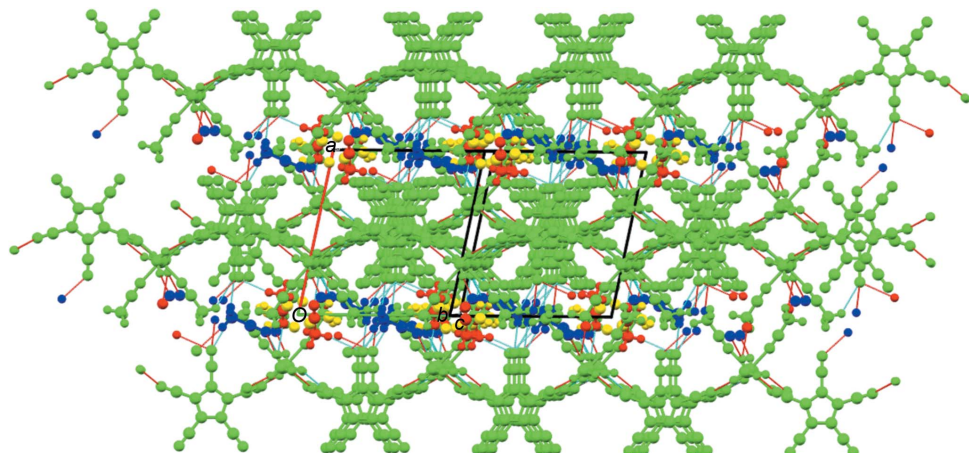
### 3. Results and discussion

The title compound crystallizes in the triclinic space group  $P\bar{1}$  with one molecule in the asymmetric unit. The  $\text{Fe}^{\text{II}}$  ion coordinates to two *cis*-oriented pentacyanocyclopentadienyl anions *via* one nitrile function each, and additionally to four acetonitrile molecules (Fig. 2).

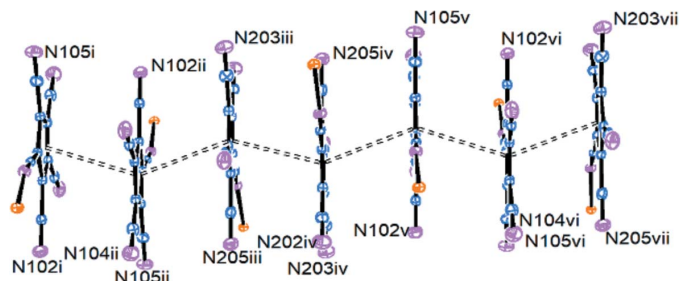
The two cyclopentadienyl rings are coplanar [interplanar angle = 0.8 (2) $^\circ$ ; the average distance of atoms C201–C205 from the best plane through C101–C105 is  $0.044 \pm 0.02$  Å].

**Figure 3**

Packing plot (*Mercury*; Macrae *et al.*, 2020), viewed along the crystallographic *a* axis. The colour coding green/blue/yellow/red corresponds to the symmetry equivalents, as defined by *Mercury*. Red and blue lines show the hydrogen bonds according to Table 4.

**Figure 4**

Packing plot (*Mercury*; Macrae *et al.*, 2020), viewed perpendicular to the *bc* plane. The colour coding is as in Fig. 3.

**Figure 5**

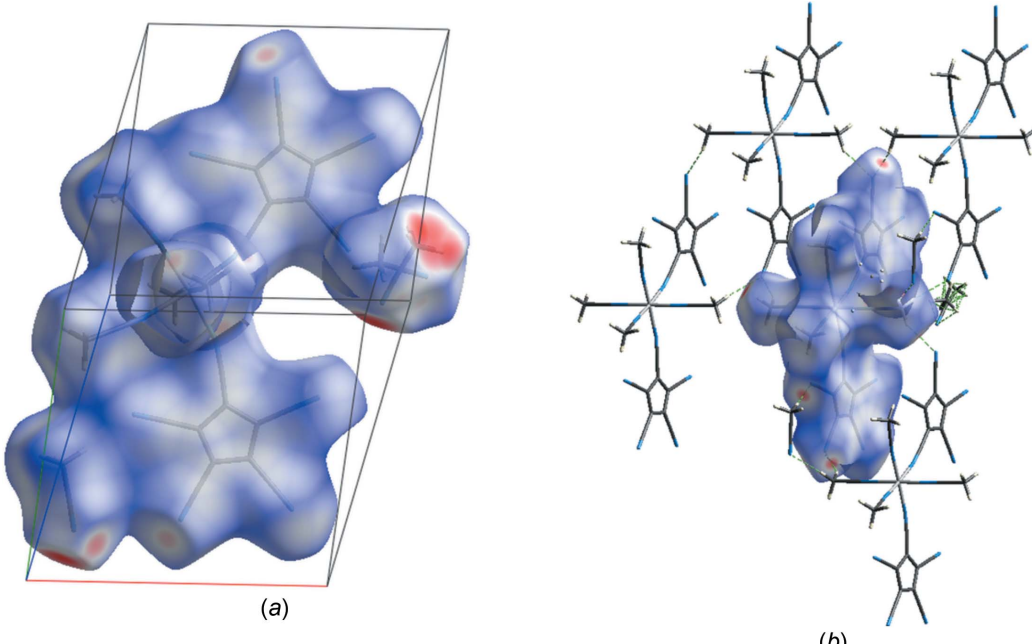
$\pi$ -Stacking of the cyclopentadienyl rings. [Symmetry codes: (i)  $x, y + 1, z - 1$ ; (ii)  $-x + 1, -y + 1, -z$ ; (iii)  $x, y, z - 1$ ; (iv)  $-x + 1, -y + 1, -z + 1$ ; (v)  $x, y, z$ ; (vi)  $-x + 1, -y, -z + 1$ ; (vii)  $x, y - 1, z$ .]

The bond lengths from the Fe atom to the  $[C_5(CN)_5]$  N atoms are significantly ( $>10\sigma$ ) longer [average 2.176 (3) Å] than to

the acetonitrile N atoms [average 2.140 (4) Å], with the bond angles at the coordinating atoms N101 and N201 close to being linear (average 161.9°). Further important bond parameters can be found in Table 3.

Weak interactions with the contents of the voids contribute to the stability of the crystal lattice (Ghosh *et al.*, 2019; Wang *et al.*, 2020) and so a closer inspection of the packing plots seemed appropriate (Fig. 3).

A packing plot viewed down the crystallographic *a* axis shows ‘layers’ of cyclopentadienyl rings oriented parallel to the *bc* diagonal and orthogonal to the plane of projection. These layers contain also one of the lattice MeCN molecules (dark blue in Fig. 3). Individual molecules are connected via C—H $\cdots$ N hydrogen bonds in the *b* and *c* directions using methyl groups C12 and C22 of the coordinated acetonitrile

**Figure 6**

(a) Hirshfeld surface of the asymmetric unit of (I) using normalized contact distances ( $d_{\text{norm}}$ ) for colour coding. Red areas represent regions where the contact distances are significantly below the sum of the van der Waals radii. (b) Hirshfeld surface of one isolated metal complex, together with some close-by neighbours, indicating also the hydrogen bridges between them and the central fragment.

**Table 3**Selected geometric parameters ( $\text{\AA}$ ,  $^\circ$ ).

Fe1—N1	2.127 (3)	Fe1—N4	2.147 (3)
Fe1—N2	2.141 (3)	Fe1—N101	2.169 (3)
Fe1—N3	2.142 (3)	Fe1—N201	2.185 (3)
N1—Fe1—N2	175.79 (12)	N101—Fe1—N201	98.60 (11)
N3—Fe1—N101	174.68 (12)	C106—N101—Fe1	162.4 (3)
N4—Fe1—N101	88.04 (12)	C206—N201—Fe1	161.2 (3)

molecules (both in *cis* positions relative to the coordinated anions) as donors and the pentacyanocyclopentadienide atoms N103 and N204 (in the 3-position relative to the coordinated cyano N atom), as well as the lattice MeCN atoms N5 and N6B, as acceptors. In addition, there is also a hydrogen bond between the lattice MeCN group C52 and pentacyanocyclopentadienide atom N102 (Table 4).

A possibly more important intermolecular interaction becomes visible in Fig. 4.

The pentacyanocyclopentadienyl rings stack *via*  $\pi$ - $\pi$  interactions (Carter-Fenk & Herbert, 2020; Thakuria *et al.*, 2019), with the ring planes at a typical distance of *ca* 3.36  $\text{\AA}$ . A closer look (Fig. 5) shows that the stack is formed by alternating pairs of inversion-related C101—C105 (symmetry codes i/ii and v/vi) and C201—C205 (iii/iv) rings. The dotted ‘bonds’ in Fig. 5 join the ring centroids at distances of 3.575 (i/ii and v/vi), 3.580 (ii/iii, iv/v and vi/vii) and 3.597  $\text{\AA}$  (iii/iv), and angles of 141.3 and 142.8°. This corresponds to a ‘ring slippage’ of *ca* 1.15  $\text{\AA}$ .

In order to gain further insight into the interactions at work, a Hirshfeld analysis was undertaken with the help of the program *CrystalExplorer* (Spackman *et al.*, 2021).

Fig. 6(a) shows the Hirshfeld surface of the asymmetric unit, with the  $d_{\text{norm}}$  surface property (range  $-0.65$  to  $1.30$ ). The strong involvement of the lattice MeCN molecules in donor C—H $\cdots$ N (top right) and acceptor N $\cdots$ H—C (bottom left) interactions can be seen. Fig. 6(b) shows the Hirshfeld surface of an isolated complex fragment and its interactions

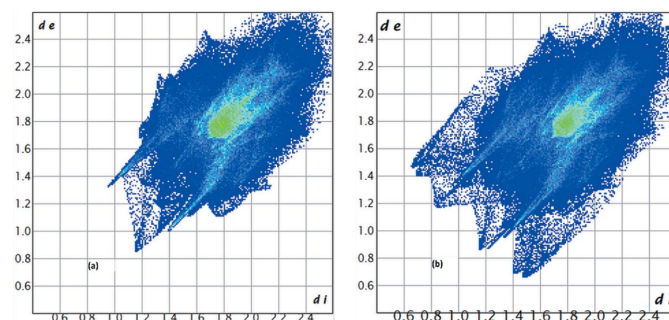
**Table 4**Hydrogen-bond geometry ( $\text{\AA}$ ,  $^\circ$ ).

$D\cdots H\cdots A$	$D—H$	$H\cdots A$	$D\cdots A$	$D—H\cdots A$
C12—H12A $\cdots$ N5A <sup>viii</sup>	0.98	2.58	3.454 (7)	149
C12—H12B $\cdots$ N103 <sup>viii</sup>	0.98	2.54	3.443 (6)	154
C12—H12C $\cdots$ N204 <sup>vii</sup>	0.98	2.56	3.469 (6)	154
C22—H22A $\cdots$ N5A <sup>ix</sup>	0.98	2.39	3.308 (7)	156
C22—H22A $\cdots$ N6B <sup>iv</sup>	0.98	2.61	3.41 (3)	138
C22—H22B $\cdots$ N204 <sup>iii</sup>	0.98	2.52	3.407 (5)	150
C22—H22C $\cdots$ N103 <sup>ix</sup>	0.98	2.52	3.424 (6)	154
C52—H52B $\cdots$ N102	0.98	2.51	3.492 (8)	176

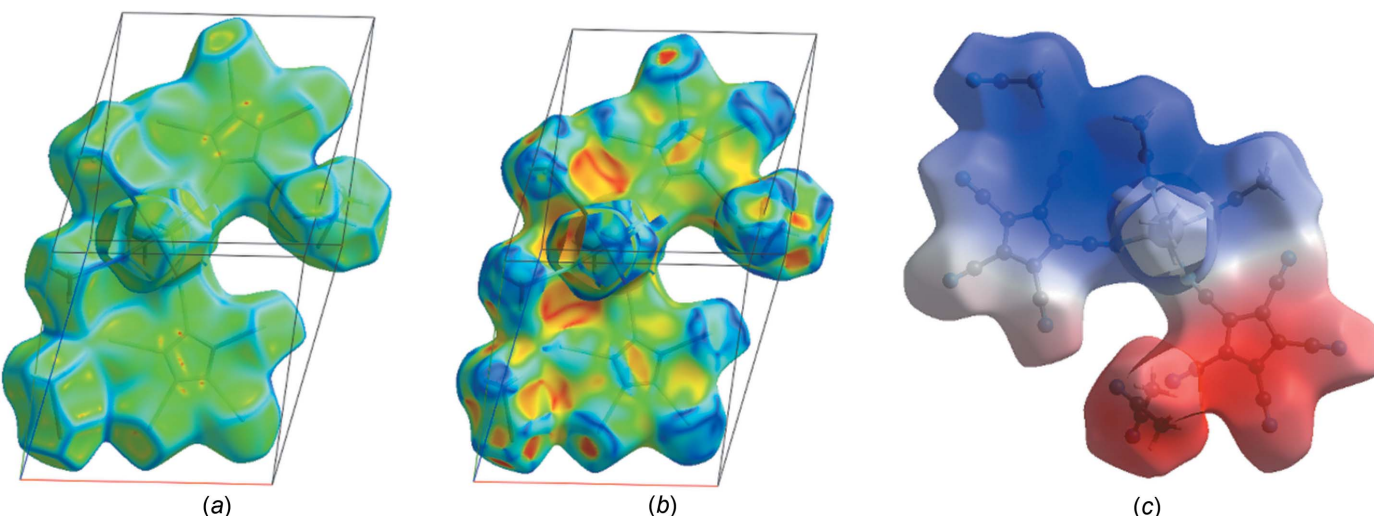
Symmetry codes: (iii)  $x, y, z - 1$ ; (iv)  $-x + 1, -y + 1, -z + 1$ ; (vii)  $x, y - 1, z$ ; (viii)  $x, y, z + 1$ ; (ix)  $x, y + 1, z$ .

with four further complex fragments and a few lattice MeCN molecules. In Fig. 7, the same surface showing the properties ‘curvedness’, ‘shape index’ and ‘electrostatic potential’ is displayed.

Both the ‘curvedness’ and the ‘shape index’ plots show the importance of planar  $\pi$ -stacking for both cyclopentadienyl rings (Spackman & Jayatilaka, 2009). Fig. 7(c) shows that the asymmetric unit contains both electropositive (blue) and electronegative (red) parts, together with small neutral (white) regions.



**Figure 8**  
Fingerprint plots (a) for a Hirshfeld surface enclosing only the iron complex and (b) for the whole asymmetric unit.

**Figure 7**

Hirshfeld surfaces displaying the properties (a) ‘curvedness’, (b) ‘shape index’ and (c) ‘electrostatic potential’.

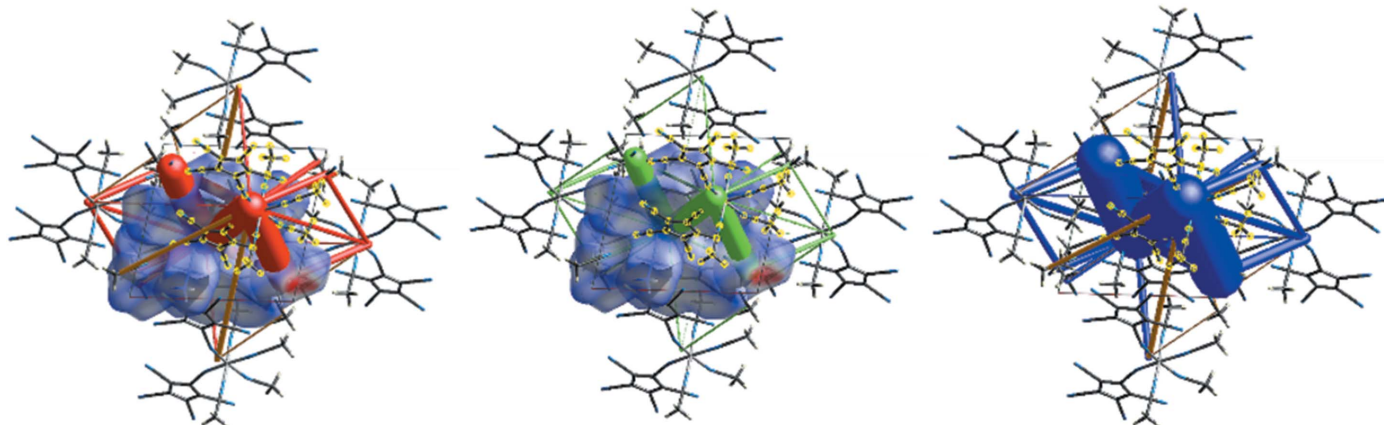


Figure 9

Energy frameworks, showing Coulombic (left) and dispersion (middle) terms, as well as total interaction energies (right).

areas. Fig. S3 (see supporting information) shows how in neighbouring molecules the positive and negative parts approach each other.

The so-called ‘fingerprints’ are a graphical representation of all the interactions of atoms ‘inside’ and ‘outside’ the Hirshfeld surface (Spackman & McKinnon, 2002). Fig. 8(a) shows such a plot when the two lattice MeCN molecules are left outside the Hirshfeld surface, while Fig. 8(b) represents such a plot when the complete asymmetric unit is inside the Hirshfeld surface. A plot showing the most important individual contributors is shown in Fig. S4 (see supporting information). The bright-green spots at *ca* (1.8/1.8) Å in Fig. 8 correspond to  $\pi\cdots\pi$  stacking interactions; inspection of Fig. S4 shows that C···C interactions are responsible for *ca* 18% of all the intermolecular interactions, while C–H··· $\pi$  interactions make up less than 7%. C–H···N contacts make up nearly 50% of the weak interactions.

A last important point relates to the interaction energies in the crystal. Fig. S5 (see supporting information) shows that the interactions between the complex and the two unique MeCN solvent molecules are relatively weak, with the repulsive terms dominating. The interactions between the asymmetric unit and four close neighbours are displayed in Fig. S6. The energies range from  $-54$  to  $-174$  kJ mol $^{-1}$ . The strongest interaction occurs for the closest approach of two inversion-related molecules (magenta), with a clear dominance of the dispersion term. Another method for graphically representing

these interactions is through the use of ‘energy frameworks’ (Turner *et al.*, 2015), which are displayed in Fig. 9.

#### 4. Conclusion

The primary reaction product from FeCl<sub>2</sub> and Ag[C<sub>5</sub>(CN)<sub>5</sub>] in acetonitrile is neither a ‘ferrocene’ nor a coordination polymer. The structure determination presented here shows a mononuclear octahedral coordination compound with two *cis*-oriented monodentate pentacyanocyclopentadienide anions and four acetonitrile ligands. The individual molecules interact in the lattice *via* weak C–H···N hydrogen bonds and displaced parallel cyclopentadienyl  $\pi$ -systems. In the absence of any crystals it is difficult to speculate about the structure of the compound ‘Fe[C<sub>5</sub>(CN)<sub>5</sub>]<sub>2</sub> $\cdot$ xH<sub>2</sub>O’ described over 50 years ago. However, one could imagine that after removal of all the acetonitrile molecules, the remaining fragments approach each other parallel to the *bc* plane and form ‘ribbons’ of Fe[C<sub>5</sub>(CN)<sub>5</sub>]<sub>4/2</sub> with the anions using two of their cyano groups, similar to the structure of Ca[C<sub>5</sub>(CN)<sub>4</sub>H]<sub>2</sub> $\cdot$ 4H<sub>2</sub>O (Sünkel & Nimax, 2018). In contrast to the Ca compound, the Fe compound would have to be octahedrally coordinated with two additional bridging H<sub>2</sub>O ligands (Fig. 10).

#### Acknowledgements

Open access funding enabled and organized by Projekt DEAL.

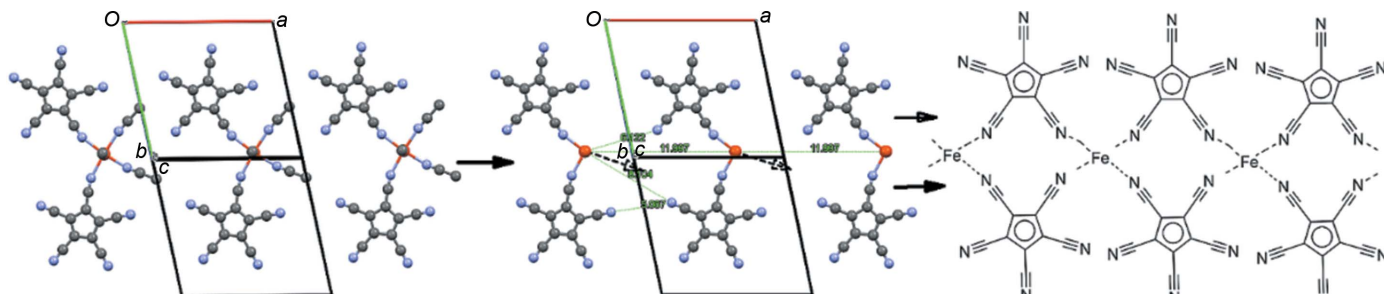


Figure 10

Suggested transformation from the title compound to a polymeric structure: (left) three molecules along the *a* direction; (middle) the same part of the structure with the MeCN molecules omitted; (right) sketch of the suggested polymer (without the bridging water ligands).

## References

- Bacsá, J., Less, R. J., Skelton, H. E., Soracevic, Z., Steiner, A., Wilson, T. C., Wood, P. T. & Wright, D. S. (2011). *Angew. Chem. Int. Ed.* **50**, 8279–8282.
- Blockhaus, T. & Sünkel, K. (2021). *Z. Anorg. Allg. Chem.* **647**, 1849–1854.
- Bruker (2011). *APEX2* and *SAINT*. Bruker AXS Inc., Madison, Wisconsin, USA.
- Carter-Fenk, K. & Herbert, J. M. (2020). *Phys. Chem. Chem. Phys.* **22**, 24870–24886.
- Christopher, R. E. & Venanzi, L. M. (1973). *Inorg. Chim. Acta*, **7**, 489–492.
- Düren, T., Millange, F., Férey, G., Walton, K. S. & Snurr, R. Q. (2007). *J. Phys. Chem. C*, **111**, 15350–15356.
- Ghosh, A. K., Hazra, A., Mondal, A. & Banerjee, P. (2019). *Inorg. Chim. Acta*, **488**, 86–119.
- Krause, L., Herbst-Irmer, R., Sheldrick, G. M. & Stalke, D. (2015). *J. Appl. Cryst.* **48**, 3–10.
- Less, R. J., Wilson, T. C., Guan, B., McPartlin, M., Steiner, A., Wood, P. T. & Wright, D. S. (2013). *Eur. J. Inorg. Chem.* **2013**, 1161–1169.
- Macrae, C. F., Sovago, I., Cottrell, S. J., Galek, P. T. A., McCabe, P., Pidcock, E., Platings, M., Shields, G. P., Stevens, J. S., Towler, M. & Wood, P. A. (2020). *J. Appl. Cryst.* **53**, 226–235.
- Nimax, P. R., Reimann, D. & Sünkel, K. (2018). *Dalton Trans.* **47**, 8476–8482.
- Sheldrick, G. M. (2015a). *Acta Cryst. A* **71**, 3–8.
- Sheldrick, G. M. (2015b). *Acta Cryst. C* **71**, 3–8.
- Spackman, M. A. & Jayatilaka, D. (2009). *CrystEngComm*, **11**, 19–32.
- Spackman, M. A. & McKinnon, J. J. (2002). *CrystEngComm*, **4**, 378–392.
- Spackman, P. R., Turner, M. J., McKinnon, J. J., Wolff, S. K., Grimwood, D. J., Jayatilaka, D. & Spackman, M. A. (2021). *J. Appl. Cryst.* **54**, 1006–1011.
- Spek, A. L. (2015). *Acta Cryst. C* **71**, 9–18.
- Spek, A. L. (2020). *Acta Cryst. E* **76**, 1–11.
- Sünkel, K. & Nimax, P. (2018). *Dalton Trans.* **47**, 409–417.
- Sünkel, K. & Reimann, D. (2013). *Z. Naturforsch. B*, **68**, 546–550.
- Sünkel, K., Reimann, D. & Nimax, P. R. (2019). *Z. Naturforsch. B*, **74**, 109–118.
- Thakuria, R., Nath, N. K. & Saha, B. K. (2019). *Cryst. Growth Des.* **19**, 523–528.
- Turner, M. J., McKinnon, J. J., Jayatilaka, D. & Spackman, M. A. (2011). *CrystEngComm*, **13**, 1804–1813.
- Turner, M. J., Thomas, S. P., Shi, M. W., Jayatilaka, D. & Spackman, M. A. (2015). *Chem. Commun.* **51**, 3735–3738.
- Wang, B., Lin, R.-B., Zhang, Z., Xiang, S. & Chen, B. (2020). *J. Am. Chem. Soc.* **142**, 14399–14416.
- Webster, O. W. (1966). *J. Am. Chem. Soc.* **88**, 4055–4060.
- Webster, O. W. (1970). US 3536694 A 19701027.
- Webster, O. W. (1974). US 3853943 A 19741210.

# supporting information

*Acta Cryst.* (2022). C78, 94–100 [https://doi.org/10.1107/S2053229622000365]

## Coordination chemistry of polynitriles. Part 9. Decacyanoferroocene revisited: crystal and molecular structure of *cis*-[ $\{\text{C}_5(\text{CN})_5\}_2(\text{MeCN})_4\text{Fe}\}$

Karlheinz Sünkel and Tobias Blockhaus

### Computing details

Data collection: *APEX2* (Bruker, 2011); cell refinement: *APEX2* (Bruker, 2011); data reduction: *SAINT* (Bruker, 2011); program(s) used to solve structure: *SHELXT2014* (Sheldrick, 2015a); program(s) used to refine structure: *SHELXL2018* (Sheldrick, 2015b); molecular graphics: *Mercury* (Macrae *et al.*, 2020); software used to prepare material for publication: *SHELXL2018* (Sheldrick, 2015b).

### Tetrakis(acetonitrile- $\kappa\text{N}$ )bis(pentacyanocyclopentadienido- $\kappa\text{N}$ )iron(II) acetonitrile disolvate

#### Crystal data

$[\text{Fe}(\text{C}_{10}\text{N}_5)_2(\text{C}_2\text{H}_3\text{N})_4] \cdot 1.8\text{C}_2\text{H}_3\text{N}$	$Z = 2$
$M_r = 674.29$	$F(000) = 696$
Triclinic, $P\bar{1}$	$D_x = 1.296 \text{ Mg m}^{-3}$
$a = 11.9972 (7) \text{ \AA}$	$\text{Mo K}\alpha$ radiation, $\lambda = 0.71073 \text{ \AA}$
$b = 12.8711 (7) \text{ \AA}$	Cell parameters from 8142 reflections
$c = 13.0907 (8) \text{ \AA}$	$\theta = 2.7\text{--}26.5^\circ$
$\alpha = 62.528 (2)^\circ$	$\mu = 0.48 \text{ mm}^{-1}$
$\beta = 82.929 (2)^\circ$	$T = 109 \text{ K}$
$\gamma = 77.210 (2)^\circ$	Block, colourless
$V = 1748.47 (18) \text{ \AA}^3$	$0.05 \times 0.04 \times 0.03 \text{ mm}$

#### Data collection

Bruker D8 Venture	17051 measured reflections
diffractometer	7081 independent reflections
Radiation source: rotating anode generator	5145 reflections with $I > 2\sigma(I)$
Detector resolution: 7.391 pixels $\text{mm}^{-1}$	$R_{\text{int}} = 0.042$
mix of $\omega$ and phi scans	$\theta_{\text{max}} = 26.4^\circ, \theta_{\text{min}} = 3.0^\circ$
Absorption correction: multi-scan	$h = -14 \rightarrow 13$
(SADABS; Krause <i>et al.</i> , 2015)	$k = -16 \rightarrow 14$
$T_{\text{min}} = 0.616, T_{\text{max}} = 0.745$	$l = -16 \rightarrow 16$

#### Refinement

Refinement on $F^2$	Hydrogen site location: inferred from
Least-squares matrix: full	neighbouring sites
$R[F^2 > 2\sigma(F^2)] = 0.064$	H-atom parameters constrained
$wR(F^2) = 0.163$	$w = 1/[\sigma^2(F_o^2) + (0.0525P)^2 + 4.4167P]$
$S = 1.02$	where $P = (F_o^2 + 2F_c^2)/3$
7081 reflections	$(\Delta/\sigma)_{\text{max}} < 0.001$
464 parameters	$\Delta\rho_{\text{max}} = 0.81 \text{ e \AA}^{-3}$
3 restraints	$\Delta\rho_{\text{min}} = -0.63 \text{ e \AA}^{-3}$
Primary atom site location: dual	

*Special details*

**Geometry.** All esds (except the esd in the dihedral angle between two l.s. planes) are estimated using the full covariance matrix. The cell esds are taken into account individually in the estimation of esds in distances, angles and torsion angles; correlations between esds in cell parameters are only used when they are defined by crystal symmetry. An approximate (isotropic) treatment of cell esds is used for estimating esds involving l.s. planes.

*Fractional atomic coordinates and isotropic or equivalent isotropic displacement parameters ( $\text{\AA}^2$ )*

	<i>x</i>	<i>y</i>	<i>z</i>	$U_{\text{iso}}^*/U_{\text{eq}}$	Occ. (<1)
Fe1	0.31525 (4)	0.41288 (5)	0.62909 (5)	0.02179 (16)	
C101	0.5159 (3)	0.1898 (3)	0.4444 (3)	0.0220 (8)	
C102	0.4447 (3)	0.1551 (3)	0.3921 (3)	0.0227 (8)	
C103	0.5156 (3)	0.0879 (3)	0.3416 (3)	0.0241 (8)	
C104	0.6307 (3)	0.0814 (3)	0.3624 (3)	0.0240 (8)	
C105	0.6311 (3)	0.1436 (3)	0.4257 (3)	0.0230 (8)	
C106	0.4747 (3)	0.2595 (3)	0.5041 (3)	0.0208 (8)	
C107	0.3223 (3)	0.1848 (3)	0.3910 (3)	0.0230 (8)	
C108	0.4783 (3)	0.0347 (3)	0.2808 (3)	0.0277 (9)	
C109	0.7278 (3)	0.0216 (3)	0.3229 (4)	0.0322 (9)	
C110	0.7303 (3)	0.1586 (3)	0.4649 (3)	0.0273 (8)	
N101	0.4360 (3)	0.3168 (3)	0.5504 (3)	0.0266 (7)	
N102	0.2255 (3)	0.2088 (3)	0.3873 (3)	0.0368 (8)	
N103	0.4496 (3)	-0.0092 (3)	0.2322 (3)	0.0411 (9)	
N104	0.8048 (3)	-0.0262 (3)	0.2907 (4)	0.0484 (10)	
N105	0.8099 (3)	0.1701 (3)	0.4953 (3)	0.0400 (9)	
C201	0.5149 (3)	0.5561 (3)	0.8071 (3)	0.0221 (8)	
C202	0.6298 (3)	0.5503 (3)	0.8270 (3)	0.0214 (7)	
C203	0.6296 (3)	0.6124 (3)	0.8915 (3)	0.0241 (8)	
C204	0.5152 (3)	0.6567 (3)	0.9116 (3)	0.0224 (8)	
C205	0.4442 (3)	0.6224 (3)	0.8594 (3)	0.0229 (8)	
C206	0.4744 (3)	0.5066 (3)	0.7450 (3)	0.0197 (7)	
C207	0.7275 (3)	0.4903 (3)	0.7878 (3)	0.0284 (9)	
C208	0.7274 (3)	0.6301 (4)	0.9295 (3)	0.0297 (9)	
C209	0.4768 (3)	0.7244 (3)	0.9745 (3)	0.0256 (8)	
C210	0.3214 (3)	0.6506 (3)	0.8589 (3)	0.0271 (8)	
N201	0.4370 (2)	0.4697 (3)	0.6948 (3)	0.0249 (7)	
N202	0.8045 (3)	0.4424 (3)	0.7558 (3)	0.0424 (9)	
N203	0.8046 (3)	0.6454 (4)	0.9608 (3)	0.0432 (9)	
N204	0.4457 (3)	0.7775 (3)	1.0254 (3)	0.0374 (8)	
N205	0.2240 (3)	0.6733 (3)	0.8597 (3)	0.0396 (9)	
C11	0.3267 (3)	0.1710 (3)	0.8712 (3)	0.0278 (8)	
C12	0.3231 (4)	0.0659 (4)	0.9790 (4)	0.0449 (11)	
H12A	0.244664	0.067321	1.010643	0.067*	
H12B	0.373736	0.064058	1.033356	0.067*	
H12C	0.348369	-0.005159	0.966392	0.067*	
N1	0.3295 (3)	0.2534 (3)	0.7868 (3)	0.0282 (7)	
C21	0.3161 (3)	0.6547 (3)	0.3858 (3)	0.0237 (8)	
C22	0.3187 (3)	0.7613 (3)	0.2786 (3)	0.0312 (9)	

H22A	0.242481	0.811730	0.264213	0.047*	
H22B	0.341848	0.739396	0.215613	0.047*	
H22C	0.373587	0.805056	0.283309	0.047*	
N2	0.3143 (2)	0.5717 (3)	0.4700 (3)	0.0221 (7)	
C31	0.1095 (3)	0.5236 (5)	0.7567 (4)	0.0414 (11)	
C32	0.0114 (4)	0.5511 (7)	0.8237 (5)	0.074 (2)	
H32A	-0.051168	0.604249	0.771923	0.111*	
H32B	0.033202	0.590484	0.864863	0.111*	
H32C	-0.013764	0.477224	0.879337	0.111*	
N3	0.1842 (3)	0.4997 (3)	0.7056 (3)	0.0312 (8)	
C41	0.1027 (3)	0.3251 (4)	0.5766 (3)	0.0318 (9)	
C42	0.0031 (4)	0.2794 (4)	0.5752 (5)	0.0534 (14)	
H42A	-0.011193	0.217475	0.652389	0.080*	
H42B	0.016765	0.245291	0.520520	0.080*	
H42C	-0.063456	0.344381	0.551764	0.080*	
N4	0.1806 (3)	0.3617 (3)	0.5788 (3)	0.0296 (7)	
C51A	0.0708 (5)	0.0441 (6)	0.2401 (6)	0.0497 (16)	0.8
C52A	0.0220 (6)	0.1035 (7)	0.3094 (7)	0.073 (2)	0.8
H52A	-0.038353	0.170740	0.266821	0.109*	0.8
H52B	0.081554	0.132953	0.327960	0.109*	0.8
H52C	-0.010596	0.047408	0.380848	0.109*	0.8
N5A	0.1071 (5)	-0.0057 (6)	0.1860 (5)	0.0666 (17)	0.8
C61A	0.9780 (6)	0.1859 (7)	0.9281 (6)	0.0515 (18)	0.8
C62A	0.8810 (6)	0.1424 (6)	0.9942 (6)	0.0573 (18)	0.8
H62A	0.868264	0.162584	1.058788	0.086*	0.8
H62B	0.894014	0.055574	1.023800	0.086*	0.8
H62C	0.813699	0.178828	0.945575	0.086*	0.8
N6A	1.0559 (6)	0.2234 (7)	0.8743 (7)	0.095 (3)	0.8
N6B	0.921 (3)	0.115 (3)	0.881 (2)	0.091 (9)*	0.2
C61B	0.944 (5)	0.147 (5)	0.944 (4)	0.095 (18)*	0.2
C62B	0.984 (3)	0.176 (3)	1.025 (3)	0.074 (9)*	0.2
H62D	0.930033	0.242670	1.030072	0.111*	0.2
H62E	0.989632	0.106186	1.100870	0.111*	0.2
H62F	1.059168	0.197529	0.999519	0.111*	0.2

*Atomic displacement parameters ( $\text{\AA}^2$ )*

	$U^{11}$	$U^{22}$	$U^{33}$	$U^{12}$	$U^{13}$	$U^{23}$
Fe1	0.0159 (3)	0.0225 (3)	0.0240 (3)	-0.00369 (19)	-0.00088 (19)	-0.0078 (2)
C101	0.0223 (18)	0.0172 (17)	0.0206 (19)	-0.0047 (14)	0.0005 (14)	-0.0034 (15)
C102	0.0221 (18)	0.0194 (17)	0.0195 (18)	-0.0068 (14)	-0.0014 (14)	-0.0013 (15)
C103	0.028 (2)	0.0203 (18)	0.0173 (18)	-0.0070 (15)	-0.0005 (14)	-0.0013 (15)
C104	0.0233 (19)	0.0186 (18)	0.0220 (19)	-0.0036 (14)	0.0009 (14)	-0.0030 (15)
C105	0.0185 (18)	0.0187 (18)	0.0240 (19)	-0.0034 (14)	-0.0006 (14)	-0.0030 (15)
C106	0.0160 (17)	0.0179 (18)	0.0221 (19)	-0.0070 (14)	-0.0029 (13)	-0.0013 (16)
C107	0.022 (2)	0.0211 (19)	0.0210 (19)	-0.0062 (14)	-0.0026 (14)	-0.0038 (16)
C108	0.031 (2)	0.022 (2)	0.022 (2)	-0.0058 (16)	-0.0009 (15)	-0.0028 (17)
C109	0.034 (2)	0.025 (2)	0.032 (2)	-0.0040 (17)	-0.0023 (17)	-0.0085 (18)

C110	0.023 (2)	0.026 (2)	0.029 (2)	-0.0016 (15)	0.0010 (15)	-0.0108 (17)
N101	0.0226 (16)	0.0238 (17)	0.0298 (18)	-0.0072 (13)	-0.0034 (13)	-0.0072 (15)
N102	0.027 (2)	0.046 (2)	0.035 (2)	-0.0076 (16)	0.0002 (14)	-0.0162 (18)
N103	0.054 (2)	0.037 (2)	0.030 (2)	-0.0131 (18)	-0.0037 (17)	-0.0108 (17)
N104	0.039 (2)	0.044 (2)	0.057 (3)	-0.0002 (18)	0.0095 (19)	-0.024 (2)
N105	0.0266 (19)	0.047 (2)	0.053 (2)	-0.0044 (16)	-0.0078 (16)	-0.027 (2)
C201	0.0260 (19)	0.0164 (17)	0.0183 (18)	-0.0061 (14)	0.0017 (14)	-0.0027 (15)
C202	0.0245 (19)	0.0172 (17)	0.0198 (18)	-0.0050 (14)	-0.0002 (14)	-0.0058 (15)
C203	0.027 (2)	0.0200 (18)	0.0209 (19)	-0.0052 (15)	0.0002 (14)	-0.0055 (16)
C204	0.031 (2)	0.0150 (17)	0.0164 (18)	-0.0040 (14)	0.0026 (14)	-0.0035 (14)
C205	0.0235 (19)	0.0173 (17)	0.0205 (18)	-0.0045 (14)	0.0018 (14)	-0.0027 (15)
C206	0.0193 (17)	0.0183 (17)	0.0174 (18)	-0.0031 (14)	0.0026 (13)	-0.0056 (15)
C207	0.030 (2)	0.028 (2)	0.028 (2)	-0.0071 (17)	-0.0042 (16)	-0.0113 (18)
C208	0.030 (2)	0.032 (2)	0.030 (2)	-0.0060 (17)	0.0047 (16)	-0.0188 (19)
C209	0.030 (2)	0.0193 (18)	0.022 (2)	-0.0046 (15)	0.0011 (15)	-0.0056 (16)
C210	0.032 (2)	0.0183 (19)	0.025 (2)	-0.0053 (15)	0.0031 (16)	-0.0054 (16)
N201	0.0195 (16)	0.0255 (16)	0.0271 (17)	-0.0039 (12)	0.0024 (12)	-0.0106 (15)
N202	0.034 (2)	0.048 (2)	0.051 (2)	0.0022 (17)	0.0027 (17)	-0.032 (2)
N203	0.034 (2)	0.055 (2)	0.052 (2)	-0.0130 (18)	0.0019 (17)	-0.033 (2)
N204	0.046 (2)	0.0296 (19)	0.035 (2)	-0.0044 (16)	0.0051 (16)	-0.0158 (17)
N205	0.029 (2)	0.037 (2)	0.051 (2)	-0.0053 (15)	0.0016 (16)	-0.0199 (19)
C11	0.027 (2)	0.028 (2)	0.030 (2)	-0.0012 (16)	-0.0035 (16)	-0.0146 (19)
C12	0.047 (3)	0.037 (3)	0.033 (3)	-0.004 (2)	-0.001 (2)	-0.002 (2)
N1	0.0305 (18)	0.0253 (18)	0.0272 (19)	-0.0033 (14)	-0.0078 (13)	-0.0096 (16)
C21	0.0157 (18)	0.030 (2)	0.028 (2)	-0.0006 (14)	0.0005 (14)	-0.0172 (19)
C22	0.034 (2)	0.026 (2)	0.028 (2)	-0.0054 (16)	0.0011 (16)	-0.0087 (18)
N2	0.0164 (15)	0.0231 (16)	0.0242 (17)	-0.0020 (12)	-0.0008 (12)	-0.0089 (15)
C31	0.021 (2)	0.070 (3)	0.041 (3)	-0.005 (2)	-0.0007 (18)	-0.033 (3)
C32	0.029 (3)	0.150 (6)	0.072 (4)	-0.008 (3)	0.005 (2)	-0.078 (4)
N3	0.0236 (18)	0.040 (2)	0.0282 (18)	-0.0073 (14)	-0.0007 (14)	-0.0127 (16)
C41	0.024 (2)	0.036 (2)	0.033 (2)	-0.0020 (17)	-0.0033 (16)	-0.0143 (19)
C42	0.030 (2)	0.050 (3)	0.077 (4)	-0.019 (2)	-0.010 (2)	-0.019 (3)
N4	0.0223 (17)	0.0348 (19)	0.0314 (19)	-0.0066 (14)	-0.0013 (13)	-0.0137 (16)
C51A	0.032 (3)	0.043 (4)	0.059 (4)	0.001 (3)	-0.006 (3)	-0.012 (3)
C52A	0.056 (4)	0.072 (5)	0.111 (7)	0.002 (4)	-0.030 (4)	-0.058 (5)
N5A	0.045 (3)	0.066 (4)	0.055 (4)	0.005 (3)	0.006 (3)	-0.007 (3)
C61A	0.033 (4)	0.042 (4)	0.053 (4)	0.011 (3)	-0.014 (3)	-0.004 (3)
C62A	0.051 (4)	0.058 (4)	0.049 (4)	-0.005 (3)	0.002 (3)	-0.015 (3)
N6A	0.049 (4)	0.099 (6)	0.095 (5)	-0.019 (4)	-0.001 (4)	-0.005 (4)

Geometric parameters ( $\text{\AA}$ ,  $^\circ$ )

Fe1—N1	2.127 (3)	C11—N1	1.128 (5)
Fe1—N2	2.141 (3)	C11—C12	1.440 (6)
Fe1—N3	2.142 (3)	C12—H12A	0.9800
Fe1—N4	2.147 (3)	C12—H12B	0.9800
Fe1—N101	2.169 (3)	C12—H12C	0.9800
Fe1—N201	2.185 (3)	C21—N2	1.129 (5)

C101—C102	1.412 (5)	C21—C22	1.444 (5)
C101—C105	1.418 (5)	C22—H22A	0.9800
C101—C106	1.420 (5)	C22—H22B	0.9800
C102—C103	1.404 (5)	C22—H22C	0.9800
C102—C107	1.433 (5)	C31—N3	1.125 (5)
C103—C104	1.416 (5)	C31—C32	1.459 (6)
C103—C108	1.423 (6)	C32—H32A	0.9800
C104—C105	1.395 (5)	C32—H32B	0.9800
C104—C109	1.427 (5)	C32—H32C	0.9800
C105—C110	1.435 (5)	C41—N4	1.145 (5)
C106—N101	1.148 (5)	C41—C42	1.450 (6)
C107—N102	1.135 (5)	C42—H42A	0.9800
C108—N103	1.148 (5)	C42—H42B	0.9800
C109—N104	1.141 (5)	C42—H42C	0.9800
C110—N105	1.142 (5)	C51A—N5A	1.149 (9)
C201—C205	1.411 (5)	C51A—C52A	1.436 (10)
C201—C202	1.413 (5)	C52A—H52A	0.9800
C201—C206	1.420 (5)	C52A—H52B	0.9800
C202—C203	1.406 (5)	C52A—H52C	0.9800
C202—C207	1.431 (5)	C61A—N6A	1.152 (9)
C203—C204	1.407 (5)	C61A—C62A	1.418 (10)
C203—C208	1.429 (5)	C62A—H62A	0.9800
C204—C205	1.406 (5)	C62A—H62B	0.9800
C204—C209	1.430 (5)	C62A—H62C	0.9800
C205—C210	1.437 (5)	N6B—C61B	1.155 (18)
C206—N201	1.146 (4)	C61B—C62B	1.430 (18)
C207—N202	1.141 (5)	C62B—H62D	0.9800
C208—N203	1.146 (5)	C62B—H62E	0.9800
C209—N204	1.138 (5)	C62B—H62F	0.9800
C210—N205	1.140 (5)		
N1—Fe1—N2	175.79 (12)	N205—C210—C205	179.1 (4)
N1—Fe1—N3	90.01 (12)	C206—N201—Fe1	161.2 (3)
N2—Fe1—N3	92.83 (12)	N1—C11—C12	179.9 (6)
N1—Fe1—N4	90.01 (12)	C11—C12—H12A	109.5
N2—Fe1—N4	93.26 (12)	C11—C12—H12B	109.5
N3—Fe1—N4	86.77 (12)	H12A—C12—H12B	109.5
N1—Fe1—N101	88.79 (12)	C11—C12—H12C	109.5
N2—Fe1—N101	88.66 (11)	H12A—C12—H12C	109.5
N3—Fe1—N101	174.68 (12)	H12B—C12—H12C	109.5
N4—Fe1—N101	88.04 (12)	C11—N1—Fe1	173.8 (3)
N1—Fe1—N201	88.02 (12)	N2—C21—C22	179.6 (4)
N2—Fe1—N201	89.04 (11)	C21—C22—H22A	109.5
N3—Fe1—N201	86.53 (12)	C21—C22—H22B	109.5
N4—Fe1—N201	173.02 (12)	H22A—C22—H22B	109.5
N101—Fe1—N201	98.60 (11)	C21—C22—H22C	109.5
C102—C101—C105	108.2 (3)	H22A—C22—H22C	109.5
C102—C101—C106	124.0 (3)	H22B—C22—H22C	109.5

C105—C101—C106	127.9 (3)	C21—N2—Fe1	178.6 (3)
C103—C102—C101	107.6 (3)	N3—C31—C32	178.2 (6)
C103—C102—C107	127.0 (3)	C31—C32—H32A	109.5
C101—C102—C107	125.4 (3)	C31—C32—H32B	109.5
C102—C103—C104	108.2 (3)	H32A—C32—H32B	109.5
C102—C103—C108	125.9 (3)	C31—C32—H32C	109.5
C104—C103—C108	125.9 (3)	H32A—C32—H32C	109.5
C105—C104—C103	108.3 (3)	H32B—C32—H32C	109.5
C105—C104—C109	127.0 (3)	C31—N3—Fe1	166.2 (4)
C103—C104—C109	124.7 (4)	N4—C41—C42	179.0 (5)
C104—C105—C101	107.8 (3)	C41—C42—H42A	109.5
C104—C105—C110	126.2 (3)	C41—C42—H42B	109.5
C101—C105—C110	126.0 (3)	H42A—C42—H42B	109.5
N101—C106—C101	176.6 (4)	C41—C42—H42C	109.5
N102—C107—C102	178.3 (4)	H42A—C42—H42C	109.5
N103—C108—C103	179.1 (4)	H42B—C42—H42C	109.5
N104—C109—C104	179.3 (5)	C41—N4—Fe1	165.3 (3)
N105—C110—C105	179.2 (4)	N5A—C51A—C52A	177.7 (8)
C106—N101—Fe1	162.4 (3)	C51A—C52A—H52A	109.5
C205—C201—C202	107.9 (3)	C51A—C52A—H52B	109.5
C205—C201—C206	124.6 (3)	H52A—C52A—H52B	109.5
C202—C201—C206	127.5 (3)	C51A—C52A—H52C	109.5
C203—C202—C201	107.9 (3)	H52A—C52A—H52C	109.5
C203—C202—C207	127.1 (3)	H52B—C52A—H52C	109.5
C201—C202—C207	125.0 (3)	N6A—C61A—C62A	178.7 (9)
C202—C203—C204	108.0 (3)	C61A—C62A—H62A	109.5
C202—C203—C208	126.7 (3)	C61A—C62A—H62B	109.5
C204—C203—C208	125.2 (3)	H62A—C62A—H62B	109.5
C205—C204—C203	108.3 (3)	C61A—C62A—H62C	109.5
C205—C204—C209	125.4 (3)	H62A—C62A—H62C	109.5
C203—C204—C209	126.3 (3)	H62B—C62A—H62C	109.5
C204—C205—C201	107.8 (3)	N6B—C61B—C62B	173 (6)
C204—C205—C210	126.0 (3)	C61B—C62B—H62D	109.5
C201—C205—C210	126.2 (3)	C61B—C62B—H62E	109.5
N201—C206—C201	177.0 (4)	H62D—C62B—H62E	109.5
N202—C207—C202	179.2 (4)	C61B—C62B—H62F	109.5
N203—C208—C203	178.8 (4)	H62D—C62B—H62F	109.5
N204—C209—C204	179.3 (4)	H62E—C62B—H62F	109.5
C105—C101—C102—C103	0.0 (4)	C205—C201—C202—C203	0.2 (4)
C106—C101—C102—C103	179.8 (3)	C206—C201—C202—C203	179.5 (3)
C105—C101—C102—C107	-179.5 (3)	C205—C201—C202—C207	179.8 (3)
C106—C101—C102—C107	0.3 (6)	C206—C201—C202—C207	-0.9 (6)
C101—C102—C103—C104	-0.2 (4)	C201—C202—C203—C204	0.0 (4)
C107—C102—C103—C104	179.4 (3)	C207—C202—C203—C204	-179.7 (3)
C101—C102—C103—C108	179.3 (3)	C201—C202—C203—C208	-179.2 (3)
C107—C102—C103—C108	-1.1 (6)	C207—C202—C203—C208	1.2 (6)
C102—C103—C104—C105	0.2 (4)	C202—C203—C204—C205	-0.2 (4)

C108—C103—C104—C105	−179.3 (3)	C208—C203—C204—C205	179.1 (3)
C102—C103—C104—C109	−179.1 (3)	C202—C203—C204—C209	179.6 (3)
C108—C103—C104—C109	1.4 (6)	C208—C203—C204—C209	−1.2 (6)
C103—C104—C105—C101	−0.2 (4)	C203—C204—C205—C201	0.3 (4)
C109—C104—C105—C101	179.1 (3)	C209—C204—C205—C201	−179.5 (3)
C103—C104—C105—C110	179.9 (3)	C203—C204—C205—C210	−179.4 (3)
C109—C104—C105—C110	−0.8 (6)	C209—C204—C205—C210	0.8 (6)
C102—C101—C105—C104	0.1 (4)	C202—C201—C205—C204	−0.3 (4)
C106—C101—C105—C104	−179.7 (3)	C206—C201—C205—C204	−179.6 (3)
C102—C101—C105—C110	−180.0 (3)	C202—C201—C205—C210	179.4 (3)
C106—C101—C105—C110	0.2 (6)	C206—C201—C205—C210	0.1 (6)

*Hydrogen-bond geometry (Å, °)*

D—H···A	D—H	H···A	D···A	D—H···A
C12—H12A···N5A <sup>i</sup>	0.98	2.58	3.454 (7)	149
C12—H12B···N103 <sup>j</sup>	0.98	2.54	3.443 (6)	154
C12—H12C···N204 <sup>ii</sup>	0.98	2.56	3.469 (6)	154
C22—H22A···N5A <sup>iii</sup>	0.98	2.39	3.308 (7)	156
C22—H22A···N6B <sup>iv</sup>	0.98	2.61	3.41 (3)	138
C22—H22B···N204 <sup>v</sup>	0.98	2.52	3.407 (5)	150
C22—H22C···N103 <sup>iii</sup>	0.98	2.52	3.424 (6)	154
C52—H52B···N102	0.98	2.51	3.492 (8)	176

Symmetry codes: (i)  $x, y, z+1$ ; (ii)  $x, y-1, z$ ; (iii)  $x, y+1, z$ ; (iv)  $-x+1, -y+1, -z+1$ ; (v)  $x, y, z-1$ .*The geometry (Å, °) around the Fe<sup>II</sup> ion*

Fe1—N101	2.170 (4)	N101—Fe1—N201	98.6 (1)
Fe1—N201	2.186 (3)	N101—Fe1—N3	174.6 (1)
Fe1—N1	2.127 (3)	N201—Fe1—N4	173.0 (1)
Fe1—N2	2.141 (3)	N1—Fe1—N2	175.8 (1)
Fe1—N3	2.143 (4)	C106—N101—Fe1	162.5 (3)
Fe1—N4	2.146 (3)	C206—N201—Fe1	161.2 (3)

*Hydrogen-bond geometry (Å, °)*

D—H···A	D—H	H···A	D···A	D—H···A
C12—H12A···N5 <sup>i</sup>	0.98	2.57	3.448	149
C12—H12B···N103 <sup>j</sup>	0.98	2.54	3.440 (5)	154
C12—H12C···N204 <sup>ii</sup>	0.98	2.57	3.469 (5)	153
C22—H22A···N5 <sup>iv</sup>	0.98	2.38	3.302	156
C22—H22A···N6B <sup>v</sup>	0.98	2.64	3.426	137
C22—H22B···N204 <sup>iii</sup>	0.98	2.53	3.406 (5)	149
C22—H22C···N103 <sup>iv</sup>	0.98	2.52	3.421 (5)	153
C52—H52B···N102	0.98	2.51	3.489	177

Symmetry codes: (i)  $x, y, z+1$ ; (ii)  $x, y-1, z$ ; (iii)  $x, y, z-1$ ; (iv)  $x, y+1, z$ ; (v)  $-x+1, -y+1, -z+1$ .